EARTHQUAKE ENGINEERING AND STRUCTURAL DYNAMICS, VOL. 25, 291–302 (1996)

DISTURBANCE REJECTION CONTROL OF BRIDGE RESPONSE TO EARTHQUAKE EXCITATION

M. S. FADALI AND K. EL-ZAYYAT
Electrical Engineering Department, University of Nevada, Reno, NV 89557-0153, U.S.A.

AND

E. MARAGAKIS
Civil Engineering Department, University of Nevada, Reno, NV 89557, U.S.A.

SUMMARY

In this paper, a new disturbance rejection controller is used to improve the response of a bridge during the application of environmental excitations. The controller combines global linearization of a non-linear bridge model and robust controller design to achieve its objectives. The resulting controller is robust with respect to disturbances, modelling errors and controller implementation errors. The method is applied to the Aptos Creek bridge in Santa Cruz under excitation caused by El-Centro earthquake.

KEY WORDS: active control; earthquake mitigation; robust control

1. INTRODUCTION

The idea of controlling or modifying the behaviour of structures under earthquakes by means of an external force is very appealing to many researchers. Since the safety of structures under abnormal conditions is critical, active control can be used successfully to suppress undesirable vibrations due to earthquakes, strong winds, etc.

The size of potential damage of a structure due to excitations can be reduced with the design of active or passive control systems.[1,2] The most popular form of passive control is base-isolation systems which reduce structural damage by earthquakes and other environmental excitations. These can be used separately or in conjunction with active controllers to form hybrid systems.

The first generation of active controllers primarily used linear models and control strategies adapted from the control literature.[3] For example, a significant body of research centered around the linear quadratic regulator (LQR) approach.[4] Modest successes were achieved, but it was soon realized that the non-linear nature of the control problem and the inaccuracies inherent in structural models demanded more sophisticated methodologies. For example, if hybrid control is used, the passive elements typically exhibit highly non-linear behaviour rendering linear designs useless.[3]

More recent research on active control has applied the H^∞ approach,[5] variable structure control[6] and intelligent control.[7] H^∞ controllers achieve performance and stability robustness using linear models but their application to non-linear models is at an early stage. Variable structure control uses switching control and often deteriorates significantly in the presence of switching delays. Intelligent control uses neural networks or fuzzy control. Neural networks have demonstrated successes as data classifiers but their application to control is still a developing research area. Fuzzy control, while easy to apply to many single-input–single-output systems, suffers from the difficulty of formulating learning rules for complex multi-input–multi-output systems.

CCC 0098–8847/96/030291–12

Received 24 June 1994
Revised 25 October 1995

The active control of the seismic response of bridges has, in general, lagged behind the active control of structures but has evolved along similar lines. Preliminary studies demonstrated the usefulness of active control of the longitudinal bridge motion both acting alone or in conjunction with passive control.[1] More recently, robust control methodologies have been successfully applied to active bridge control.[8]

In this paper, a new active control methodology based on global linearization[9,10] and disturbance rejection[11] is introduced. Earthquake force is modelled as an external disturbance with given upper bound, and variations in the model parameters are accounted for in the controller design. A simple but adequate discrete model is used to represent bridge dynamics. The design methodology is used to design a controller based on this model and on the spectrum of the worst-case disturbance. The new methodology is then applied to Aptos Creek bridge, a structure in Santa Cruz, California. The control system is evaluated by simulating the response of the bridge to the 1979 El-Centro earthquake.

The outline of this paper is as follows. Section 2 reviews the idea of global linearization. Section 3 discusses disturbance rejection control design. Section 4 outlines the design procedure for the new methodology. To illustrate the application of the methodology, the control of the seismic response of Aptos Creek bridge is given in Section 5. Conclusions and observations are given in Section 6.

2. GLOBAL LINEARIZATION

Global linearization for non-linear control system design has been successfully applied to many control problems.[12,13] The main advantage of this approach is that non-linear system dynamics can be mapped to equivalent linear dynamics for design purposes. The designer can thus apply linear design methodologies to obtain the desired time response. The non-linear system controller can then be obtained from the linear system controller so that the non-linear system follows the desired linear dynamics.[14]

Consider a non-linear system of the form

$$\ddot{x} = -A_1 x - A_2 \dot{x} + f(x, \dot{x}) + B(x, \dot{x})u \tag{1}$$

where x is a $n \times 1$ vector of generalized coordinates, u is a $n \times 1$ control vector, $f(x, \dot{x})$ is a $n \times 1$ vector and $B(x, \dot{x})$ is a $n \times n$ matrix. The entries of the vector $f(x, \dot{x})$ and the matrix $B(x, \dot{x})$ are non-linear functions of the co-ordinates x and the velocities $\dot{x}$. This model includes lumped (discrete) models of bridges and robotic manipulators, among others.

For any model of the form (1), a globally equivalent linear model can be obtained by simply redefining the input vector as $v := \ddot{x} + A_1 x + A_2 \dot{x}$. Hence, the system reduces to the linear dynamics

$$\ddot{x} + A_2 \dot{x} + A_1 x = v \tag{2}$$

The linear input v can be chosen as the state feedback

$$v = -K_1 x_1 - K_2 x_2 \tag{3}$$

where $A_i + K_i, i = 1, 2$ are positive definite to guarantee system stability.[14] The physical input to the non-linear system can be calculated using

$$u = B^{-1}(x, \dot{x})[v - f(x, \dot{x})] \tag{4}$$

assuming invertible $B(x, \dot{x})$ for all feasible co-ordinates x. Alternatively, a dynamic output feedback controller can be used to determine v from the state $(x, \dot{x})$ as shown in Figure 1. Note that the dynamic relationship between x and v is linear and can be described by an s-domain transfer function $P(s)$ but the control u is non-linear.

The main drawback of this methodology is that the accuracy of our estimate of u depends on the accuracy of the system parameters that appear in A_1, A_2, $B(x, \dot{x})$ and $f(x, \dot{x})$. Thus the controller selected for this system must be robust with respect to modelling errors. This, and other limitations of global linearization, is discussed in the tutorial.[12] In the next section, we present a methodology for the design of a robust controller to be used with global linearization.

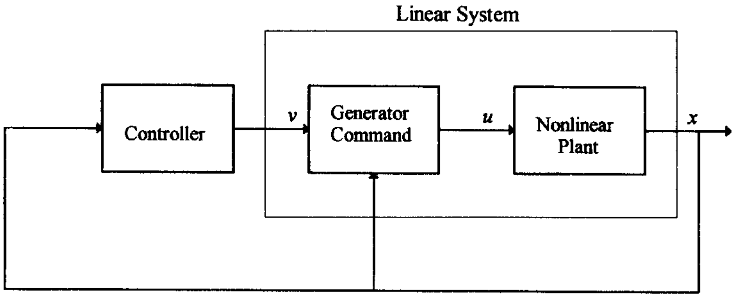

Figure 1. Block diagram for global linearization

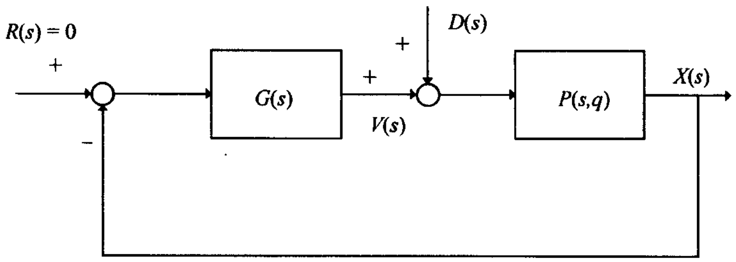

Figure 2. Block diagram of closed-loop unity feedback system with cascade compensation

3. DISTURBANCE REJECTION CONTROL MODELS

Consider the model given in Figure 2 where $P(s, q)$ is the transfer function of the globally linearized structure, $G(s)$ is the controller to be determined, $X(s)$ are the generalized co-ordinates, $D(s)$ is an $l \times 1$ vector of disturbances (earthquake accelerations in this case) and q is a $p \times 1$ vector of uncertain plant parameters. For example, the entries of q may occur in the intervals $[q_{i-}, q_{i+}]$, $i = 1, 2, \ldots, p$.

The overall disturbance transfer function $T_D(s)$ is given by

$$X(s) = T_D(s, q)\,D(s) = [I + P(s, q)\,G(s)]^{-1}\,P(s, q)\,D(s)$$
$$= [P^{-1}(s, q) + G(s)]^{-1}\,D(s) \tag{5}$$

The ith co-ordinate is related to the jth disturbance, $j = 1, \ldots, l$, by

$$X_i(s) = \sum_{j=1}^{l} T_{D_{ij}}(s, q)\,D_j(s) \tag{6}$$

where T_{Dij} is the ijth entry of the matrix $T_D(s, q)$. For the response to the disturbance to remain below a specified level, we require

$$|P^{-1} + G|_{ij} < B_{Dij} \tag{7}$$

where $|\cdot|_{ij}$ denotes the absolute value of the ijth matrix entry.

By examining the spectrum of worst-case disturbances $D_{ij}(j\omega)$, a suitable transfer function model $T_{Dij}(j\omega, q)$, $i, j = 1, \ldots, n$, can be selected for disturbance rejection. For example, $T_{Dij}(j\omega, q)$ can be selected as a low-pass filter for high frequency disturbances, a high-pass filter for low frequency disturbances and so forth. Hence, the bounds $B_{Dij}(j\omega)$ can be obtained for all frequencies ω and for all transfer functions $T_{Dij}(j\omega, q)$. A suitable controller G can then be selected to satisfy (7) given the family of transfer functions $P(j\omega, q)$. The process is considerably simpler in the case of a diagonal matrix $T_{Dij}(j\omega, q)$ i.e. $T_{Dij}(j\omega, q) = 0$, $i \neq j$, $i = 1, \ldots, n$.

4. DESIGN PROCEDURE

A methodology for active bridge control to reject earthquake disturbances can be formulated based on the theoretical development of Sections 2 and 3. The methodology requires the non-linear modelling of the bridge, global linearization of the non-linear model and disturbance rejection design for the linear equations. The controller design is completed using the following procedure:

1. Obtain a non-linear lumped model for the bridge structure and write its non-linear differential equations of motion.
2. Obtain the globally linearized description of the structure and determine its transfer function.
3. Obtain the discrete Fourier transform of a worst-case record of the disturbance and use the spectrum to define a suitable disturbance rejection model.
4. Using the methodology of Section 3, design a compensator to satisfy the disturbance rejection requirement (7) for the disturbance rejection model obtained in Step 3.
5. Check the design using computer simulation and repeat Steps 4 and 5 if necessary, until the results indicate sufficient disturbance rejection with feasible control forces.

5. DESIGN EXAMPLE

The Aptos Creek bridge is located approximately six miles east of Santa Cruz on California Highway 1. A simplified picture of the bridge is shown in Figure 3. The bridge has an intermediate expansion joint located at the left of bent angle.

A simplified lumped model of the longitudinal displacement of Aptos Creek bridge is shown in Figure 4. The model includes two masses m_1, m_2, to represent the bridge deck on both sides of the expansion joint and

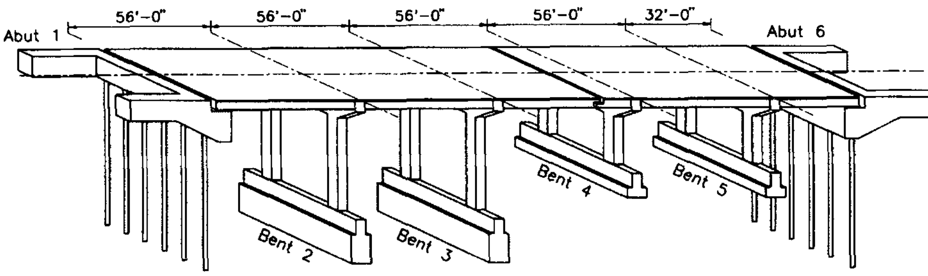

Figure 3. Aptos Creek bridge model (1 ft = 0·3048 m)

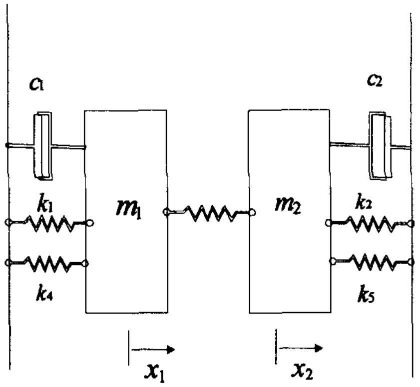

Figure 4. Lumped model of Aptos Creek bridge

springs k_1, k_2, to represent the stiffness of the abutments. The support columns are modelled as springs k_4, k_5, and dampers c_1, c_2. A non-linear spring force f_c represents the force of the restraining cables of the middle expansion part. Throughout this study, spring hysteresis is neglected for simplicity but the non-linear nature of the restraining cable is accounted for in the design. The model was validated using a finite element model developed in recent studies[16] of the Aptos Creek bridge assuming linear springs. The finite element program SAP90 results closely resembled the results obtained for the discrete model used here.

The equations of motion for the system in the longitudinal direction under earthquake excitation are expressed as

$$m_1\ddot{x}_1 + c_1\dot{x}_1 + (k_1 + k_4)x_1 + f_c(x_1, x_2) = f_1 - f_e \tag{8}$$

$$m_2\ddot{x}_2 + c_2\dot{x}_2 + (k_2 + k_5)x_2 - f_c(x_1, x_2) = f_2 - f_e \tag{9}$$

where

m_1, m_2:	masses of bridge girder
k_1, k_2, k_4, k_5:	stiffness coefficients
c_1, c_2:	damping coefficients
x_1:	relative displacement with respect to m_1
x_2:	relative displacement with respect to m_2
f_1:	control force applied to m_1
f_2:	control force applied to m_2
f_e:	earthquake force

f_c is the non-linear spring force between the two masses and is given by

$$f_c(x_1, x_2) = \begin{cases} q, & \Delta x > 0 \\ 0, & \varepsilon < \Delta x < 0 \\ \infty, & \Delta x < \varepsilon \end{cases} \tag{10}$$

where q is a constant, ε is the gap between the two masses, and Δx is the relative distance between the two masses, i.e.

$$\Delta x = \varepsilon + (x_2 - x_1) \tag{11}$$

Equations (8) and (9) can be rewritten as

$$\ddot{x}_1 = -\frac{c_1}{m_1}\dot{x}_1 - \left(\frac{k_1 + k_4}{m_1}\right)x_1 - \frac{f_c(x_1, x_2)}{m_1} + \frac{f_1}{m_1} - \frac{f_e}{m_1} + \Delta f_1(x_1, x_2) \tag{12}$$

$$\ddot{x}_2 = -\frac{c_2}{m_2}\dot{x}_2 - \left(\frac{k_1 + k_4}{m_2}\right)x_2 - \frac{f_c(x_1, x_2)}{m_2} + \frac{f_2}{m_2} - \frac{f_e}{m_2} + \Delta f_2(x_1, x_2) \tag{13}$$

to include bounded modelling errors Δf_1 and Δf_2. To obtain the globally linearized model, the linear system inputs v_1, v_2, are defined as

$$v_1 = -\frac{f_c(x_1\ x_2)}{m_1} + \frac{f_1}{m_1} \tag{14}$$

$$v_2 = \frac{f_c(x_1, x_2)}{m_2} + \frac{f_2}{m_2} \tag{15}$$

The corresponding controller forces are

$$f_1 = m_1 v_1 + f_c(x_1, x_2) \tag{16}$$

$$f_2 = m_2 v_2 - f_c(x_1, x_2) \tag{17}$$

Table I. Parameter values of the Aptos Creek Bridge

Parameter	m_1 ($\times 10^3$ kg)	m_2 ($\times 10^3$ kg)	k_1 (kN/m)	k_2 (kN/m)	k_4 (kN/m)	k_5 (kN/m)
Value	204·2	141·7	$1{\cdot}2\times 10^6$	$1{\cdot}2\times 10^6$	6×10^4	$4{\cdot}9\times 10^5$

The values of the parameters of Aptos Creek bridge are given in Table I. We assume a damping ratio $\zeta \in [0{\cdot}05, 0{\cdot}15]$ and equal damper constants c_1 and c_2. For an equivalent bridge damper constant c, we have the relationship

$$\zeta = \frac{c}{2m_{eq}\,\omega_n} \tag{18}$$

where ω_n is the natural frequency of the bridge given by

$$\omega_n^2 = \frac{k_{eq}}{m_{eq}} \tag{19}$$

Substituting from Table 1 gives the equivalent mass

$$m_{eq} = m_1 + m_2 = 345{\cdot}9 \times 10^3 \text{ kg}$$

and equivalent spring

$$k_{eq} = k_1 + k_2 + k_4 + k_5 = 2{,}950{,}000 \text{ kN/m}$$

Hence, the natural frequency $\omega_n = 92{\cdot}350$ rad/s, and, for a nominal damping ratio $\zeta = 0{\cdot}05$, the damping constant $c = 3194{\cdot}378$ and $c_1 = c_2 = c/2 = 1597{\cdot}189$ kN s/m. The nominal equations of motion excluding non-linear modelling errors and disturbances are

$$\ddot{x}_1 = -7{\cdot}822\dot{x}_1 - 6170{\cdot}421x_1 - \frac{f_c(x_1, x_2)}{204{\cdot}2} + \frac{f_1}{204{\cdot}2} \tag{20}$$

$$\ddot{x}_1 = -11{\cdot}272\dot{x}_2 - 38814{\cdot}397x_2 + \frac{f_c(x_1, x_2)}{141{\cdot}7} + \frac{f_2}{141{\cdot}7} \tag{21}$$

The transfer function for each mass is found using equations (12)–(15) with the disturbances and modelling errors set equal to zero. Hence, we have

$$P_1(s) = \frac{X_1(s)}{V_1(s)} = \frac{1}{m_1 s^2 + c_1 s + k_1 + k_4}$$

for the first mass, and

$$P_2(s) = \frac{X_2(s)}{V_2(s)} = \frac{1}{m_2 s^2 + c_2 s + k_2 + k_5}$$

for the second mass. The actual parameters values for m_i, $i = 1, 2$, and k_i, $i = 1, 2, 4, 5$, are assumed to be within 10% of their nominal values. The actual values for c_i, $i = 1, 2$, are assumed to be in the range corresponding to $\zeta \in [0{\cdot}05, 0{\cdot}15]$.

Next, we examine the acceleration time history for the El-Centro earthquake shown in Figure 5. The acceleration data is discrete Fourier transformed to obtain the spectrum of Figure 6. Figure 6 shows that the earthquake spectrum has significant components at low frequencies. The bridge acts as a low pass filter in that it does not respond to high frequency components. Hence, a band-pass filter with gain below unity in the pass band is an acceptable choice of disturbance transfer function to reject the earthquake disturbance.

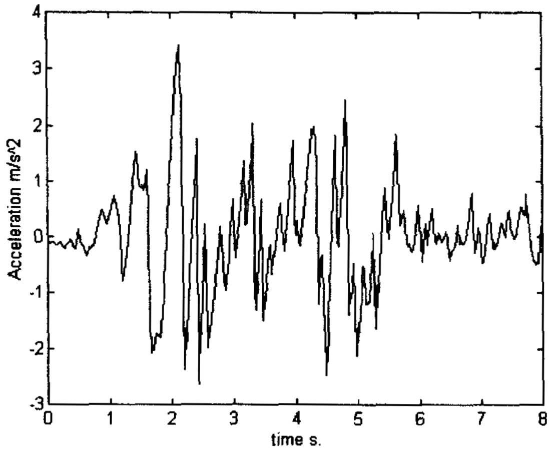

Figure 5. El-Centro earthquake time data history

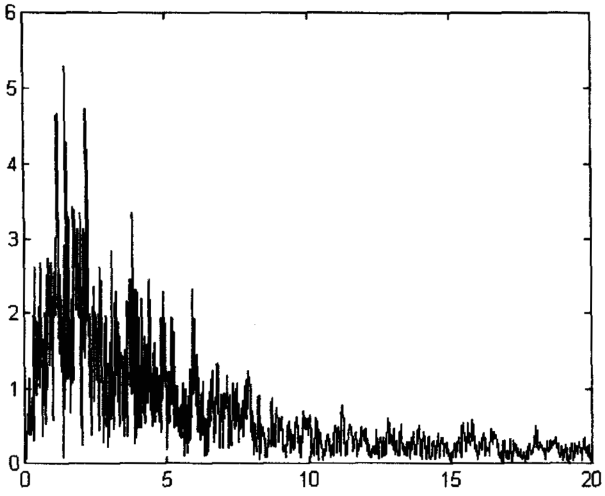

Figure 6. Spectrum of the time history of El-Centro earthquake

The disturbance transfer function $T_D(s)$ is selected as

$$T_D(s) = \frac{0{\cdot}1(3{\cdot}33s + 1)}{(0{\cdot}2s + 1)(0{\cdot}1s + 1)}$$

A controller is selected for each mass to satisfy the disturbance rejection bounds. The controller that satisfies the bounds for the first mass m_1 is

$$G_1 = \frac{(20s + 1)(3{\cdot}33s + 1)}{(0{\cdot}2s + 1)(0{\cdot}125s + 1)^2}$$

and for the second mass m_2

$$G_2 = \frac{(50s + 1)(3{\cdot}33s + 1)}{(0.25s + 1)(0{\cdot}166s + 1)(0{\cdot}1s + 1)}$$

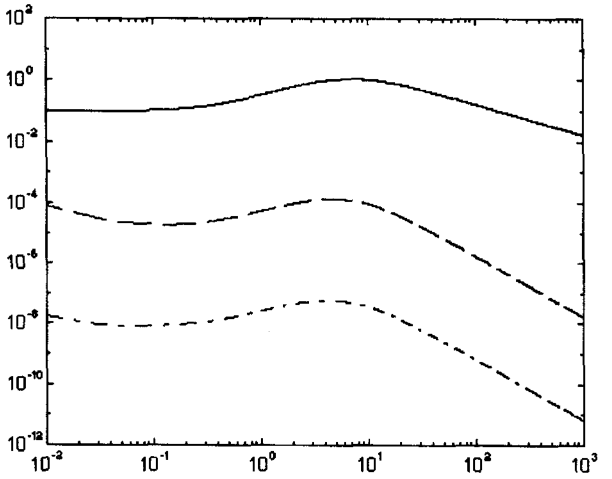

Figure 7. Selected disturbance transfer function model T_d (———) and actual closed-loop transfer functions from m_1 (– –) and m_2 (· – ·) (Design I)

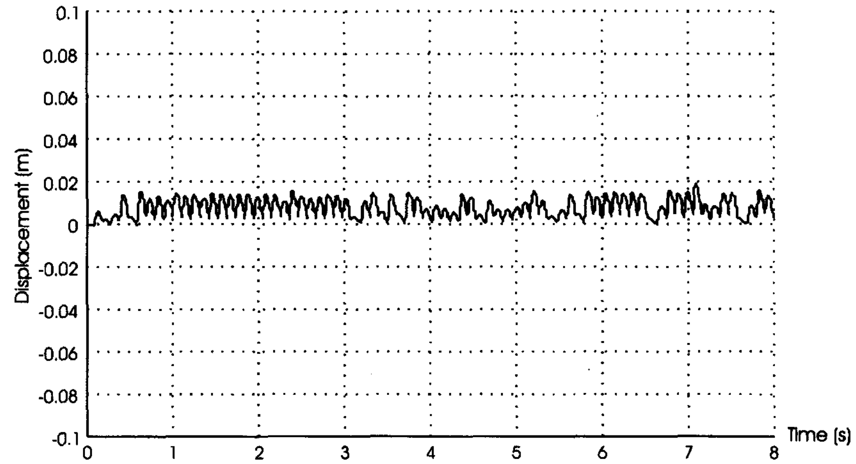

Figure 8. Displacement of m_1 with active control (Design I)

The closed-loop frequency responses for m_1 and m_2 are shown in Figure 7 together with the frequency response $T_D(j\omega)$ which defines the bounds $B_D(j\omega)$. They represent band-pass filters and meet the rejection model requirements. This design is referred to in the sequel as Design I.

The software package SIMULINK* was used to simulate the bridge with and without active control. Figures 8 and 9 show the corresponding time histories under the disturbance rejection active control for masses m_1 and m_2, respectively. The control forces applied to masses m_1 and m_2 are shown in Figure 10 and 11, respectively.

The results show that with peak control forces of 115 kN for the first mass and 101 kN for the second, the displacements are less than 0·018 m for deck 1 and less than 0·009 m for deck 2. By contrast, the result with no active control (omitted for brevity) have peak displacements of 0·2 and 0·14 m for decks 1 and 2, respectively. Clearly, such a large displacement will not occur in practice where the bridge will fail due to the earthquake. This is because the simple model used here is not valid for large displacements. Nevertheless, the simulations

*SIMULINK is a simulation package of MATHWORKS, Inc. of Natick, Massachusetts.

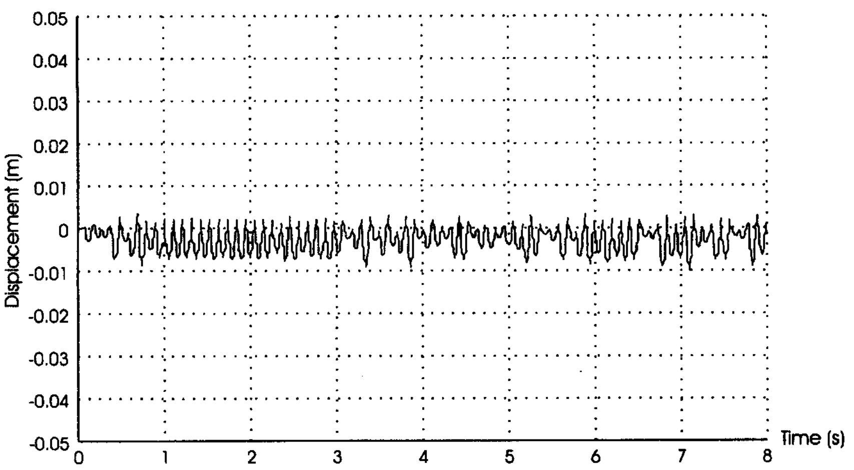

Figure 9. Displacement of m_2 with active control (Design I)

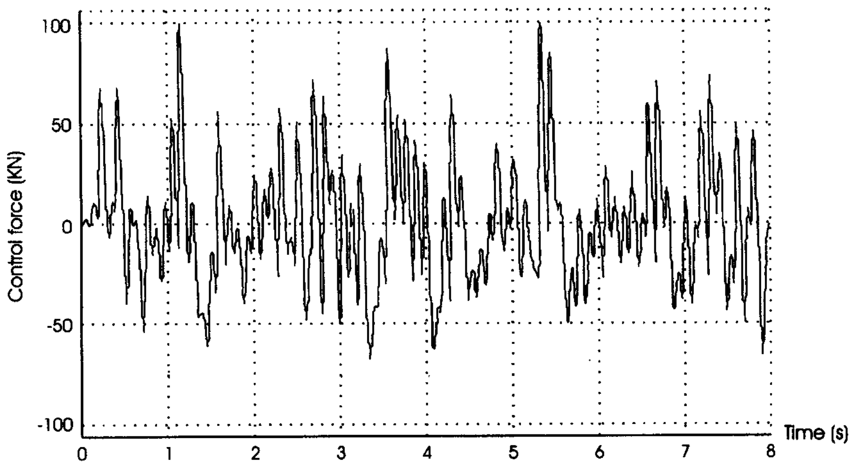

Figure 10. Control force applied to m_1 (Design I)

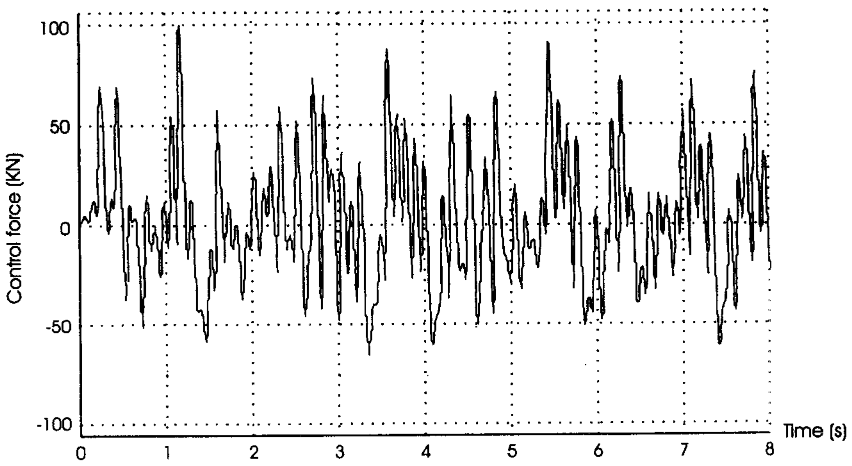

Figure 11. Control force applied to m_2 (Design I)

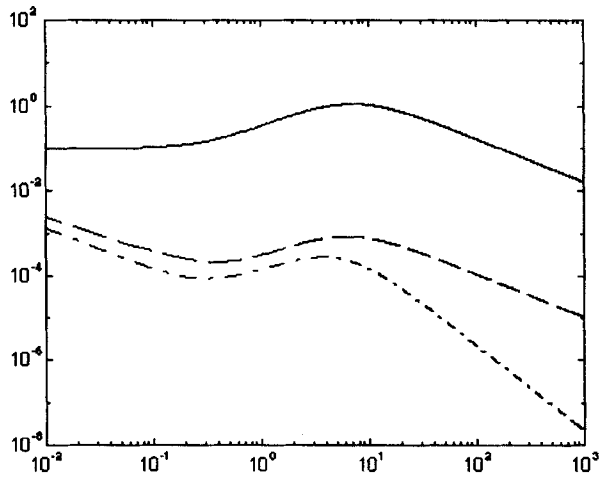

Figure 12. Selected disturbance transfer function model T_d (———) and actual closed-loop transfer functions for m_1 (– –) and m_2 (. – .) (Design II)

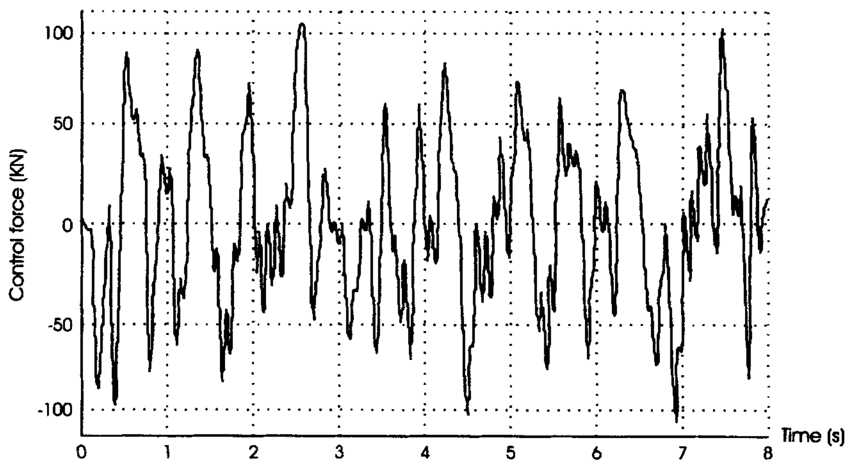

Figure 13. Control force applied to m_1 (Design II)

indicate the destructive effect of the earthquake on the bridge structure in the absence of active control. The simulation results of Figures 8 and 9 are more accurate since they correspond to small displacements under which the model validity was verified using SAP90.

If necessary, it is possible to reduce the magnitude of the active control by redesigning the controller. A second design (referred to as Design II) allows a significant reduction in the force magnitude by more closely adhering to the bounds $B_D(j\omega)$. The controller transfer functions for Design II are

$$G_1 = \frac{29{\cdot}8(2s+1)(19s+1)(3{\cdot}33s+1)}{(11s+1)(0{\cdot}2s+1)(0{\cdot}125s+1)^2}$$

$$G_2 = \frac{21{\cdot}3(13s+1)(2{\cdot}5s+1)(4s+1)}{(12s+1)(0{\cdot}25s+1)(0{\cdot}166s+1)(0{\cdot}15s+1)}$$

with $G_i(s)$ the controller for m_i, $i = 1, 2$. The controllers yield disturbance rejection transfer functions that satisfy the specified bounds as shown in Figure 12. The corresponding control forces are shown in Figures 13

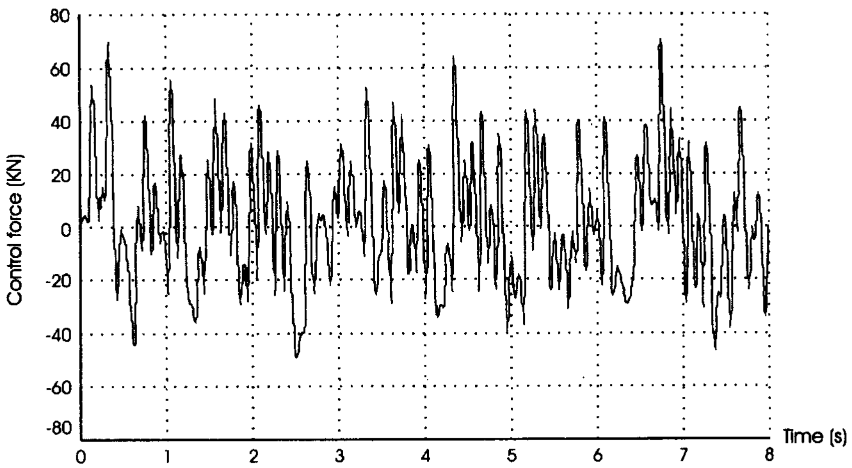

Figure 14. Control force applied to m_2 (Design II)

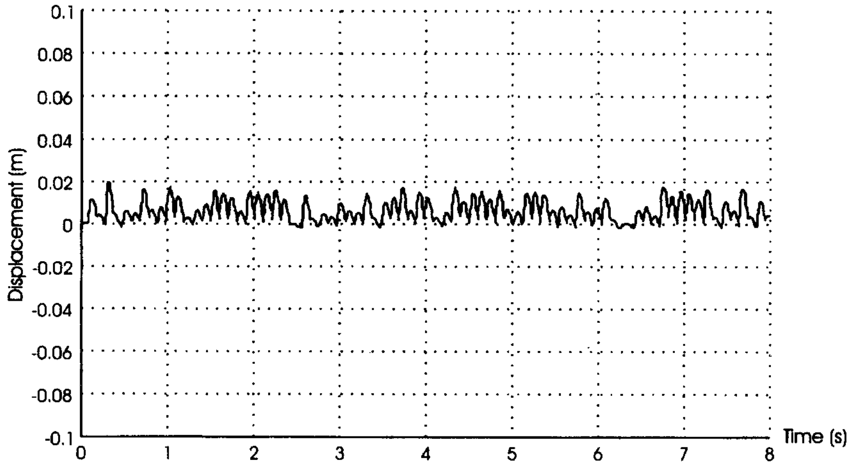

Figure 15. Displacement of m_1 with active control (Design II)

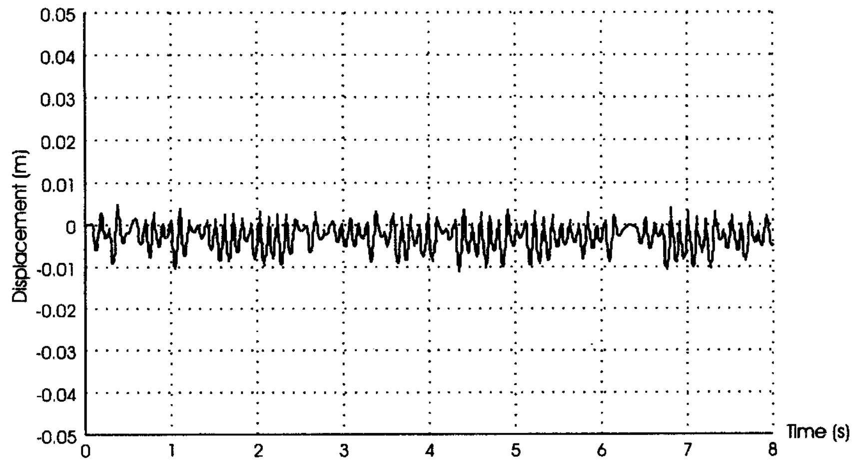

Figure 16. Displacement of m_2 with active control (Design II)

and 14, respectively. The forces have a peak value of 102 kN for m_1 and 70 kN for m_2. This represents a reduction in the peak force magnitude of about 15 per cent. The displacements for m_1 and m_2 are shown in Figures 15 and 16, respectively. The peak displacements for Design II are 0·021 m for m_1 and 0·013 m for m_2.

6. CONCLUSION

Global linearization and disturbance rejection control were used to reduce the displacement of a bridge under earthquake excitations. Simulation results show that the proposed design significantly reduces the effect of earthquakes on structures. The finite element program SAP90 was used to confirm the simulation results for the linear case.

Two controller designs were completed for the bridge. Design I demonstrated that the bridge deck displacements can be reduced to less that 0·015 m with the use of sufficiently large control forces. Design II demonstrated that even with the reduction of controller force by about 15 per cent, the bridge deck displacements can be reduced to less than 0·022 m. In practice, the final design must be a compromise between reduction of displacements and the magnitude of the required control forces.

Spring hysteresis and other non-linearities were not considered in this study for simplicity. However, non-linear decoupling can be used to linearize models including these non-linearities to allow disturbance rejection controller design. The forces required may increase slightly above the level encountered here. Considering the fact that the peak forces needed for disturbance rejection in the bridge example here were below those used in other studies,[2] it is expected that the increase in force needed to handle the non-linearities will remain acceptable.

The model considered here accounted for earthquake excitation in the longitudinal direction only. Excitation in other directions, including coupling between lateral and longitudinal excitation, may occur in practice. More complex bridge models are required to account for these excitations but the design methodology presented here can be used with minor modifications.

ACKNOWLEDGEMENT

The authors would like to thank Dr. S. Abdel-Ghaffar, Dr. M. El-Gamal and Dr. S. Feng for providing data and assistance with bridge modelling and simulation.

REFERENCES

1. M. Abdel-Rohman and H. H. Leipholz, 'Active control of flexible structures', *J. eng. struct. ASCE* **104**, 1251–1266 (1990).
2. I. D. Aiken, D. K. Nims and J. M. Kelly, 'Comparative study of four passive energy dissipation systems', *Bull. N.Z. nat. soc. earthquake eng.* **25**, 3 (1992).
3. G. W. Housner, T. T. Soong and S. F. Masri, 'Second generation of active structural control in civil engineering', *Proc. first world congress on structural control*, Panel 3-15, Los Angeles, CA, 1994.
4. C. P. Pantelides, 'Computer-controlled structure', *J. comput. struct. ASCE* **34**, 715–725 (1990).
5. S. F. Masri, G. Bekey and T. Caughey, 'Optimum pulse control of flexible structures', *J. appl. mech. ASME* **48**, 619–626 (1981).
6. S. F. Masri, R. K. Miller, T. J. Dehghenyar and T. Caughey, 'Active parameter control of nonlinear vibrating structures', *J. appl. mech. ASME* **56**, 658–666 (1989).
7. A. Joghataie and J. Ghaboussi, 'Neural networks and fuzzy logic in structural control', *Proc. first world congress on structural control*, WP1 21-30, Los Angeles, CA, 1994.
8. W. Xu, S. F. Masri and B. Yang, 'Modeling and control of a distributed system under non-uniform support excitation', *Proc. first world congress on structural control*, FA1 39-48, Los Angeles, CA, 1994.
9. H. Nijmeijer and A. J. Van der Schaft, *Nonlinear Dynamical Control Systems*, Springer, New York, 1990.
10. A. Isidori, *Nonlinear Control Systems*, Springer, Heidelberg, 1989.
11. J. J. D'Azzo and C. H. Houpis, *Linear Control System Analysis and Design*, McGraw-Hill, New York, 1988.
12. M. S. Fadali, 'Continuous drug system design using nonlinear decoupling: a tutorial', *IEEE trans. bio-medical eng.* **34**, 650–653 (1989).
13. B. Jakubczyk and W. Respondek, 'On linearization of control systems' *Bull. acad. polonaise sci. ser. sci.* Math. **28**, 517–522 (1980).
14. J. E. Slotine and W. Li, *Applied Nonlinear Control*, Prentice-Hall, Englewood Cliffs, New Jersey, 1991.
15. M. Horowitz, *Synthesis of Feedback Systems*, Academic Press, Orlando, FL, 1963.
16. S. Abdel-Ghaffar and E. Maragakis, 'Aptos Creek bridge design', A paper presented at U.S.–Japan Conference at Lake Tahoe (1992).